Expl Agric. (2018), volume 54 (4), pp. 604–622 © *Cambridge University Press 2017*
doi:10.1017/S0014479717000278

RELIABILITY OF NDVI DERIVED BY HIGH RESOLUTION SATELLITE AND UAV COMPARED TO IN-FIELD METHODS FOR THE EVALUATION OF EARLY CROP N STATUS AND GRAIN YIELD IN WHEAT

By PAOLO BENINCASA†‡, SARA ANTOGNELLI†, LUCA BRUNETTI†, CARLO ALBERTO FABBRI§, ANTONIO NATALE§, VELIA SARTORETTI§, GIANLUCA MODEO§, MARCELLO GUIDUCCI†, FRANCESCO TEI† *and* MARCO VIZZARI†

†*Department of Agricultural, Food and Environmental Sciences, University of Perugia, Borgo XX Giugno, 74, 06121, Perugia, Italy and* §*TeamDev – Software, GIS and Web Engineering – Via Tiberina, 70, 06050, Perugia, Collepepe di Collazzone, Italy*

(*Accepted 8 May 2017*; *First published online 6 June 2017*)

SUMMARY

This study was aimed at comparing in-field parameters and remote sensing NDVI (normalized difference vegetation index) by both satellite (SAT) and unmanned aerial vehicle (UAV) for the assessment of early nitrogen (N) status and prediction of yield in winter wheat (*Triticum aestivum* L.). Six increasing N rates, i.e., 0, 40, 80, 120, 160, 200 kg N ha^{-1} were applied, half at tillering and half at shooting. Thus, when the crop N status was monitored between the two N applications, consecutive N treatments differentiated from each other by just 20 kg N ha^{-1}. The following in-field and remote sensed parameters were compared as indicators of crop vegetative and N status: plant N% (w:w) concentration; crop N uptake (Nupt); ratio between transmitted and incident photosynthetically active radiation (PARt/PARi); leaf SPAD values, an indirect index for chlorophyll content; SAT and UAV derived NDVI. As reliable indicators of wheat N availability, in-field parameters were ranked as follows: PARt/PARi ≅ Nupt > SPAD ≅ N%. The PARt/PARi, Nupt and SPAD resulted quite strongly correlated to each other. At all crop stages, the NDVI was strongly correlated with PARt/PARi and Nupt. It is of relevance that NDVI correlated quite strongly to in-field parameters and grain yield at shooting, i.e., before the second N application, when the N rate can still be adjusted. The SAT and UAV NDVIs were strongly correlated to each other, which means they can be used alternatively depending on the context.

INTRODUCTION

Economic and environmental sustainability of cropping systems can be improved by reducing inputs (i.e., tillage, irrigation water and fertilizers, pesticides and herbicides) and increasing use efficiencies. This implies the adoption of precision agriculture practices (Bongiovanni and Lowenberg-Deboer, 2004; Bora *et al.*, 2012). In few words any input should be provided at the right rate (neither less, to avoid yield loss, nor more, to avoid money loss, pollution and health risks), at the right time (i.e., synchronizing application schedule with crop needs) and only where necessary

‡Corresponding author. Email: paolo.benincasa@unipg.it

(i.e., targeted delivery), as revealed by an accurate monitoring of the crop status. As far as nitrogen (N) fertilization is concerned, the total N rate should be defined with due accuracy because it is the main factor affecting N use efficiency and thus the chance to obtain high yield with limited N loss to the environment (Muñoz-Huerta *et al.*, 2013). A balance approach is required, based on estimated total crop N need and estimated amounts of N available in the soil at sowing (N_{min}) and of N that will become available during the growing cycle. The total N rate is then likely to be split into several applications in order to reduce leaching risks, allowing in-season adjustments of the N rate according to the actual crop N status. In fact, initial estimates of total N rates may fail due to unpredictable season weather and soil variability between fields or field patches. For this reason, a monitoring of the crop N status is needed over time and space, in particular in early growth phases, when any adjustment of the crop N status can still be effective for the final yield.

The absolute reference to evaluate the crop nutritional status is the critical N concentration, i.e., the minimum N concentration needed in plant tissues to maximize crop growth and yield. The critical N concentration is known to decrease along the crop growing cycle according to a so called critical N dilution curve, as reported for wheat by Cao *et al.* (2015). At any growth stage, there is a critical N concentration below which the crop would yield less than potential, and over which the crop would have luxury N accumulation (Tei *et al.*, 2003). Therefore, lab analyses on destructive plant samples could reveal the actual N status of the crop, but they are not feasible in the ordinary farm practice, because labour consuming, expensive and not timely. Alternative quick tests have been proposed for in-field destructive or non-destructive monitoring of the crop N status, e.g., chlorophyll meter readings (SPAD), VIS–NIR spectroscopy, and nitrate-N concentration in the petiole sap (sap test) (Muñoz-Huerta *et al.*, 2013; Ulissi *et al.*, 2011). The accuracy of these methods has been found to be quite high, although variable with the species and the crop N status. A feasible alternative to in-field monitoring for crop N status on medium and large scale is the use of vegetation indices (VIs) calculated through proximal or remote sensing of canopy spectral response in the wavelength of green, red, red-edge and near infrared using multispectral sensors (Cao *et al.*, 2015; Maresma *et al.*, 2016).

Despite the wide range of VIs available in the literature, the most widespread VI for assessing vegetation status remains the normalized difference vegetation index (NDVI) (Basso *et al.*, 2001), largely used as a reference index in many papers comparing VIs and sensors (Cao *et al.*, 2015; Huete *et al.*, 1997; Thenkabail *et al.*, 2000). The NDVI usually varies between −1 (water) and +1 (dense and vigorous vegetation). NDVI can be easily calculated by proximal sensor measurements (Casa and Castrignanò, 2008; Quebrajo *et al.*, 2015; Tilling *et al.*, 2007), however, these methods are still labour consuming for representative plant sampling and thus hard to use for monitoring spatial heterogeneity of the crop in wide fields. NDVI calculation using remote-sensed images can represent an alternative to proximity methods, giving the chance to easily get quantitative information over time and space. Remote multi-spectral sensors are able to measure canopy reflectance in R and NIR bands allowing NDVI calculation over larger areas. Depending on the specific application, sensors can be carried at

https://doi.org/10.1017/S0014479717000278 Published online by Cambridge University Press

different altitudes by satellites (SAT), airplanes, helicopters and by different types of unmanned aerial vehicles (UAV) flying at low altitude.

SAT images, due to the acquisition heights, are generally characterized by a coarser resolution, but a higher applicability to wide area observations, and so, they are able to recognize variation in vegetation growth, and to support N management at district or regional level (Huete *et al.*, 1997; Wu *et al.*, 2015). On the other hand, Low Altitude Remote Sensing (LARS) using UAV includes a range of data collection techniques operating through different sensors (mainly optical) commonly applied in precision agriculture (Maresma *et al.*, 2016; Torres-Sánchez *et al.*, 2014). These techniques are suitable when traditional remote sensing cannot be applied (e.g., cloudy skies, small fields, requirement of higher resolution maps). While NDVI from SAT images (SAT NDVI) is typically calculated using reflectance values after radiometric and atmospheric corrections (Campbell and Wayne, 2011), NDVI from UAV images (UAV NDVI) is generally calculated after a calibration based on different approaches as single or multiple reflectance calibration targets and incident light sensors (Candiago *et al.*, 2015; Honkavaara *et al.*, 2014; Saberioon *et al.*, 2014)

Winter wheat is a typical crop where the N rate is split in at least two application times in order to increase N uptake efficiency, support the formation of yield components and limit N leaching by fall-spring rainfall. The first N application usually falls in late fall-early winter, while the last occurs in late winter-early spring. Therefore, there is room to evaluate the crop N status after the first N application and, in case, adjust the rate by the following fertilizer application in order to avoid yield loss or overfertilization. This would be of great relevance as wheat is the most widespread crop all over the world and Mediterranean rainfed cropping systems are actually based on winter wheat (Benincasa *et al.*, 2016; Bonciarelli *et al.*, 2016). The accuracy of crop N status evaluation in early growth stages becomes crucial for this purpose. To this aim, remote sensing methods could be very useful for overcoming all the issues depicted above for in-field and proximal methods. SAT and UAV NDVI have been widely tested to assess wheat N status and estimate crop final yield, with encouraging results. Strong correlations were found between SAT NDVI and specific agronomic traits such as above ground biomass (Perry *et al* 2013), SPAD, stem sap nitrate, biomass and N uptake (Jia *et al* 2012) as well as between UAV NDVI and wheat leaf area index (Lelong *et al.*, 2008). However, few studies compared lab analysis on plant samples and in-field and remote sensing methods to assess wheat N status in early growth stages (Cao *et al.*, 2015; Eitel *et al.*, 2011; Perry *et al.*, 2013). None of these studies compared both SAT and UAV NDVIs although SAT and UAV images generally differ in terms of spatial, spectral and radiometric resolution, and pre-processing procedures applied on them. Moreover, wheat N availabilities differed widely due to differences in N rates and/or spreading techniques (Cao *et al.*, 2015; Eitel *et al.*, 2011; Sultana *et al.*, 2014).

Hence, the aim of this work was to compare in-field parameters and the widely used NDVI, evaluating the reliability of NDVI through UAV and SAT remote sensing for detecting small differences in wheat early N status and predicting yield.

MATERIALS AND METHODS

Crop and treatments

The experiment was carried out at the Foundation for Agricultural Education of the University of Perugia, located in Casalina, Province of Perugia, middle Tiber valley, Central Italy (170 m a.s.l., 42.95°N, 12.40°E). The field was located in a plain area characterized by a rather homogeneous loam soil with 1.3% (w:w) organic matter. Winter wheat (*Triticum aestivum* L., cv. PRR58) was sown on November 24th, 2014 at the density of 400 seeds m^{-2} in rows 0.125 m apart. Experimental treatments consisted of six increasing fertilizer-N rates: 0, 40, 80, 120, 160 and 200 kg N ha^{-1} as urea, split into two applications of half rate each, the first at tillering (February 12th, 2015, i.e., 80 days after sowing, DAS) and the second at shooting (April 14th, 2015, i.e., 141 DAS). Treatments were laid down in a randomized blocks design with three replicates, with a total of 18 plots. Each plot measured 78 m^2 (6 × 13 m), with the main axis oriented North–South.

In-field measurements

Growth analysis and N accumulation. Plant samplings were taken on February 12th (80 DAS), i.e., just before the first fertilizer-N application; April 14th (141 DAS), i.e., about two months after the first N application and just before the second N application; May 17th (174 DAS), i.e., about one month after the second N application. At each sampling date, all plants (roots excluded) from 0.375 m^2 per plot (i.e., 0.5 m per row in six central rows) were harvested to measure the fresh (FW, Mg ha^{-1}) and dry (DW, Mg ha^{-1}) weights after 72 h at 80 °C. The N concentration (N%) of grinded subsamples of the dry matter was measured by the Kjeldahl method (TKN, Total Kjeldahl Nitrogen). The total N accumulation in the above ground biomass (Nupt, kg ha^{-1}) was calculated as the product of DW by N concentration.

SPAD readings. The SPAD 502 (Minolta Ltd., Osaka, Japan) is a portable spectrophotometer for in-field non-destructive quick measurements of leaf greenness, which is correlated to chlorophyll concentration, and in turn, with N concentration in leaf tissues (Hoel and Solhaug, 1998). SPAD measurements were performed several times between tillering and initial grain filling: January 28th (65 DAS); February 12th (80 DAS); March 4th (100 DAS) and 19th (115 DAS); April 1st (128 DAS) and 29th (156 DAS); May 13th (170 DAS) and 27th (184 DAS). In every date, measurements were taken on ten top fully expanded leaves (then the flag leaf, after heading) from 10 plants per plot.

Measurements of photosynthetically active radiation. The PAR incoming upon the canopy (PARi) and transmitted to the soil below the canopy (PARt) was measured with a ceptometer (AccuPAR PAR-80, Decagon Devices Inc., Pullman, WA, USA) in order to calculate the PARt/PARi ratio. The measurements were performed on April 1st (128 DAS) and 29th (156 DAS) and on May 13th (170 DAS). At each measurement

https://doi.org/10.1017/S0014479717000278 Published online by Cambridge University Press

date, five PARt measurements were taken per plot, by positioning the line ceptometer normal to wheat rows direction.

Grain yield. Wheat grain yield (GY, Mg ha^{-1}) was determined for each plot by harvesting the whole plot area excluding two border rows per side. The thousand grain weight (TGW, g) was determined based on the dry weight of three replicates of 100 grains each.

NDVI from satellite data (SAT NDVI)

SAT NDVI was calculated using two high resolution multi-spectral images. The first was collected on March 18th, 2015 (114 DAS) by the GeoEye-1 satellite including blue (450–510 nm), green (510–580 nm), red (655–690 nm) and near infrared (780–920 nm) bands. The second was collected on May 10th, 2015 (167 DAS) by the WorldView-2 satellite including blue (400–450 nm), green (506–586 nm), red (624–694 nm), and near infrared (765–901 nm) bands. The spatial resolution at ground level was 2 m and the radiometric resolution 11 bit (2048 levels for each band). Both the images were geometrically and atmospherically corrected using GRASS GIS modules with the purpose of reducing the deformations produced by the terrain morphology, the atmosphere and lighting conditions on the values measured by the two satellite sensors. Geometric correction was performed by an orthorectification procedure using a 10 m resolution DTM (Digital Terrain Model), while the atmospheric correction was based on the application of the 6S algorithm (Second Simulation of Satellite Signal in the Solar Spectrum) (Vermote *et al.*, 1997) on radiance at top-of-atmosphere (TOA) values. With the aim to improve the direct comparison of NDVI values calculated from remote-sensed data from different satellites, a further co-registration procedure was developed, based on the NDVI calculated on pseudo-invariant sites (Bouvet, 2014). These sites were identified through the selection of 32 points located on objects whose ground reflectance does not change significantly over time, such as paved roads, roofs, and other pseudo-invariant surfaces (Hadjimitsis *et al.*, 2009). The average responses of red and near infrared bands (NIR) in circular areas of 5 m radius around the points were calculated, and then a linear regression between average values was performed. The R^2 value of the red and NIR spectral bands between the two satellite images was 0.91 and 0.90, respectively. These correlation values indirectly highlighted a difference between the reflectance curves, which justified the application of this additional calibration procedure. The linear regression allowed the coefficients calculation to calibrate the Geo-Eye 1 image on the WorldView2 image. After being cross-calibrated using QGIS (QGIS Development Team 2014), the red and NIR bands were used to calculate NDVI (Supplementary Figure S1 available online at http://dx.doi.org/10.1017/S0014479717000278), as NDVI = (NIR –R)/(NIR+R), where NIR is the reflectance in the near-infrared portion of the EM spectrum and R is the reflectance in the red portion of the EM spectrum.

Wheat growth stage is a very important factor influencing NDVI response (Hansen and Schjoerring, 2003). Thus, in order to perform a chronologically effective comparison between satellite, UAV, and in-field data, we estimated the satellite NDVI values on April 14th, 2015 (141 DAS, shooting) by a linear interpolation between available satellite NDVI data on March 18th (114 DAS) and May 10th (167 DAS). The linear approach appears reliable as NDVI values have been demonstrated to grow linearly from early tillering to booting growth stage (De la Casa and Ovando, 2013; Perry *et al.*, 2013). The final NDVI mean values were calculated using the grid statistics for polygon QGIS tool on the SAT NDVI layers and parcel geometries, excluding an internal buffer of 1 m to limit boundary effects.

NDVI from UAV data (UAV NDVI)

The UAV data collection was performed through a compact, light and robust carbon hesacopter (SF6, Skyrobotic, Italy) equipped with a stable flight controller and a multispectral camera (ADC Micro, Tetracam, Inc., CA, USA) detecting green (520–600 nm), red (630–690 nm), and NIR (760–900 nm) bands. The camera sensor, 6.55 × 4.92 mm wide, with a pixel size of 3.2 μm and a focal length of 8.43 mm, is able to produce images of 2048 × 1536 pixels. Flight height was set to 100 m above ground with an average flight speed of 5 m s^{-1}. Thanks to the gimbal system, the camera was able to collect stable and nadiral images with a spatial resolution of 3.8 cm. All the shoots were on-fly georeferenced by the NRTK (Network Real Time Kinematic) technique, based on the reception of differential correction data in real time from a permanent stations network through the NTRIP protocol. UAV images were collected on three dates: March 31st (127 DAS), April 14th (141 DAS, i.e., about two months after the first N application and just before the second N application), and May 18th (175 DAS, i.e., about one month after the second N application). Raw images were pre-processed and radiometrically corrected using the Tetracam PixelWrench II software (Company, Country). Calibration coefficients were calculated by the software using a picture taken before the flight on the white Teflon calibration tag supplied with the camera. Processed images were subsequently rectified, mosaicked, and georeferenced using the Agisoft Photoscan software (Company, Country). Twelve Ground Control Points (GCPs), georeferenced using a dual-frequency NRTK GNSS receiver, were used to improve spatial accuracy of final image mosaics. NDVI calculation was performed in QGIS using red and NIR bands from final image mosaics (Figure S1). Also in this case, the NDVI mean values were calculated for each date using the grid statistics for polygon QGIS tool on the UAV NDVI raster layers and parcel geometries, excluding an internal buffer of 1 m to limit border effects.

Data analysis

In order to assess the efficacy of SAT and UAV data for revealing N crop status, linear correlation coefficients were calculated between either SAT NDVI or UAV NDVI and parameters from in-field measurements performed both in early and

https://doi.org/10.1017/S0014479717000278 Published online by Cambridge University Press

late growth stages. Due to weather and/or logistical aspects (i.e., rainfall and field accessibility, need to respect fertilization schedule, need of clear sky with no passage of clouds, high ratio of direct/diffuse radiation, and no or slow wind), in-field measurements and image acquisitions were not always synchronous. In particular, frequent cloudy weather and rainfall (about 170 mm) occurred between February 20th and April 10th, particularly during the whole month of March (150 mm), which hampered/delayed the second N application and many of in-field measurements. However, comparable data were collected through these measurements. A time schedule of cultivation operations and measurements during the wheat growing cycle is reported in Figure S2.

RESULTS

In-field data

All parameters from in-field measurements (FW, DW, N%, Nupt, SPAD, PARt/PARi) varied with fertilizer-N rate and crop stage (Figure 1). In particular, FW, DW and N uptake increased while PARt/PARi decreased with either increasing N rate or crop ageing. On the other hand, N% and SPAD values generally increased with N rate and decreased with crop ageing (except for SPAD at later dates and at high N rates). All treatments showed N% concentration in the dry matter always below the critical N concentration reported by Cao *et al.* (2015) (Figure 2).

Pairwise linear correlations between Nupt and PARt/PARi, SPAD and N%, SPAD and Nupt (i.e., the independent parameters more linked to crop N nutrition and leaf development) are reported for either just before (141 DAS) and after (170 DAS) the second N application (Figure 3). No correlations can be drawn for measurements in March in lack of most of in field parameters for that period. The correlations were less strong before than after the second N application. The correlation was significant and strong between PARt/PARi and Nupt and between Nupt and SPAD in both crop stages (Figure 3A,C,D,F). The correlation between N% and SPAD was significant but weak in the first crop stage and became moderate only in the second one (Figure 3B,E).

Wheat grain yield (GY) increased with increasing N rate, but differences between the highest N rates were slight and generally not significant (Table 1). The thousand grain weight decreased slightly at high N rates (Table 1).

Remote sensed NDVI

Both SAT and UAV NDVI values were affected by wheat N availability, but differences were not always significant between N rates over 80 kg N ha^{-1} (Figure 4). The SAT and UAV NDVIs were strongly correlated in all the three crop stages, with R^2 increasing from 0.84 at the second half of March (around 120 DAS) to 0.90 in mid-April (about 140 DAS) and 0.95 around mid-May (around 170 DAS) (Figure 5). On April 14th (141 DAS, i.e., just before the second N application), pairwise correlation of UAV NDVI versus in-field parameters were always stronger than those of SAT NDVI (Table 2). The strongest correlations were those of UAV NDVI versus Nupt

https://doi.org/10.1017/S0014479717000278 Published online by Cambridge University Press

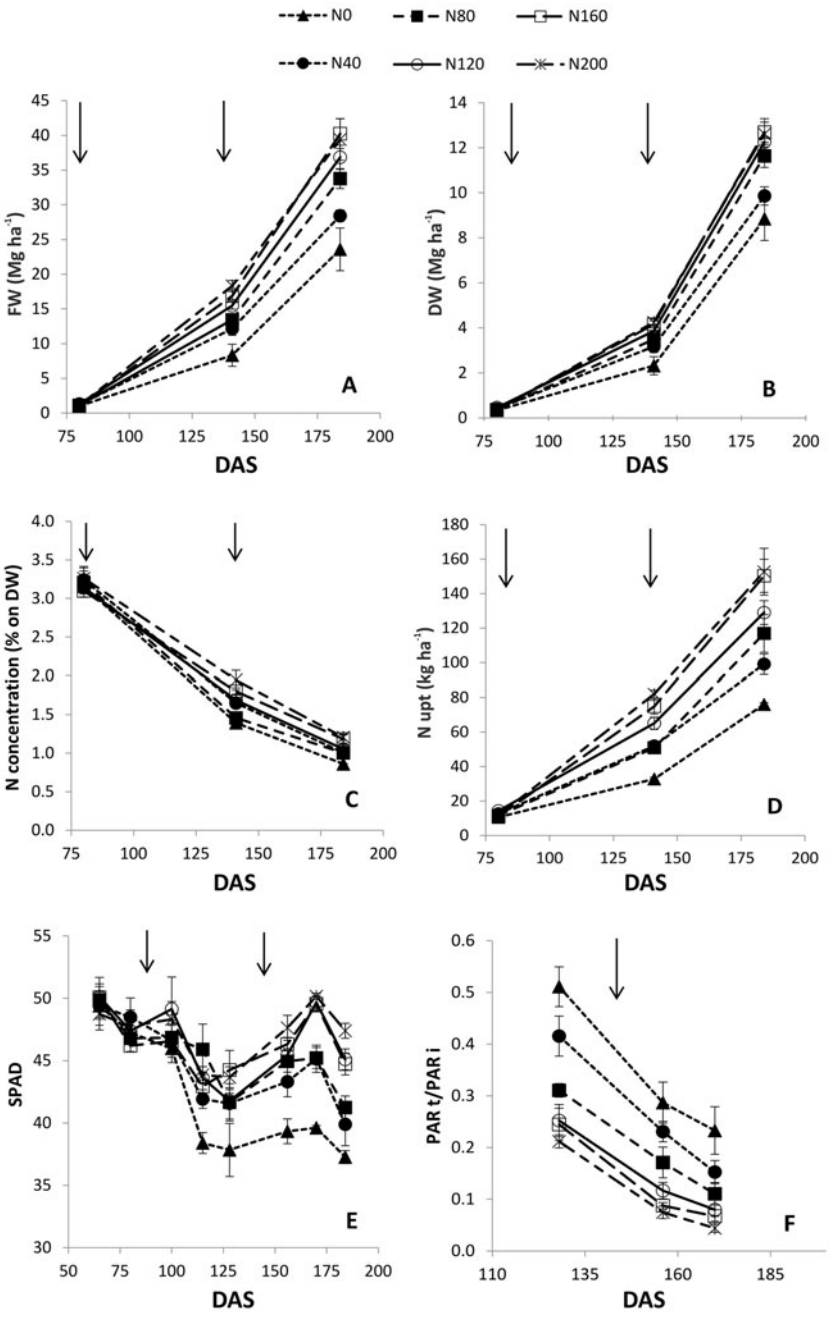

Figure 1. Time course of above ground biomass fresh weight (FW, in A) and dry weight (DW, in B), N% concentration (C), total above-ground N accumulation (Nupt, in D), SPAD values (i.e., greenness) of leaves (E), and PARt/PARi ratio (F) in soft wheat as affected by increasing N fertilization rates (0, 40, 80, 120, 160, 200 kg N ha^{-1}), split into two applications (see arrows), the first at tillering (February 12th, 2015, 80 days after sowing, DAS) and the second at shooting (April 14th, 2015, 141 DAS). PARt is the photosynthetically active radiation transmitted to the soil below the canopy and PARi the PAR incoming above the canopy. Vertical bars represent standard errors.

https://doi.org/10.1017/S0014479717000278 Published online by Cambridge University Press

Table 1. Grain yield (GY) and thousand grain weight (TGW) in soft wheat grown at increasing N fertilization rates (0, 40, 80, 120, 160, 200 kg N ha^{-1}), split into two applications, the first at tillering (February 12th, 2015, 80 days after sowing, DAS), the second at shooting (April 14th, 2015, 141 DAS).

N rate	GY	TGW
kg N ha^{-1}	Mg DW ha^{-1}	g
0	4.5	4.9
40	5.7	5.0
80	5.9	5.0
120	7.8	4.8
160	8.3	4.5
200	8.4	4.6
Mean	6.8	4.8
AnOVa	***	***
LSD $p = 0.05$	0.97	0.15

*** = Fisher's significance at $p < 0.001$.

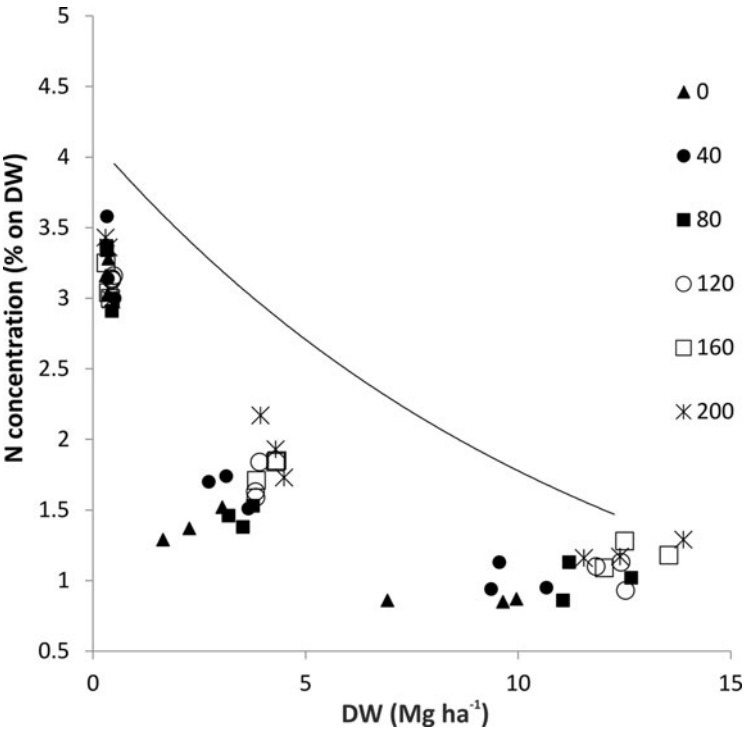

Figure 2. Correlation between N% concentration (on above-ground dry biomass) and above-ground biomass (DW) observed in wheat grown at increasing N fertilization rates (0, 40, 80, 120, 160, 200 kg N ha^{-1}), split into two applications, the first at tillering (February 12th, 2015, 80 days after sowing, DAS) and the second at shooting (April 14th, 2015, 141 DAS). The symbols represent the data collected from each plot at the sampling dates of February 12th, April 14th and May 17th (174 DAS), and the curve represents the critical N concentration for wheat by Cao *et al.* (2015).

https://doi.org/10.1017/S0014479717000278 Published online by Cambridge University Press

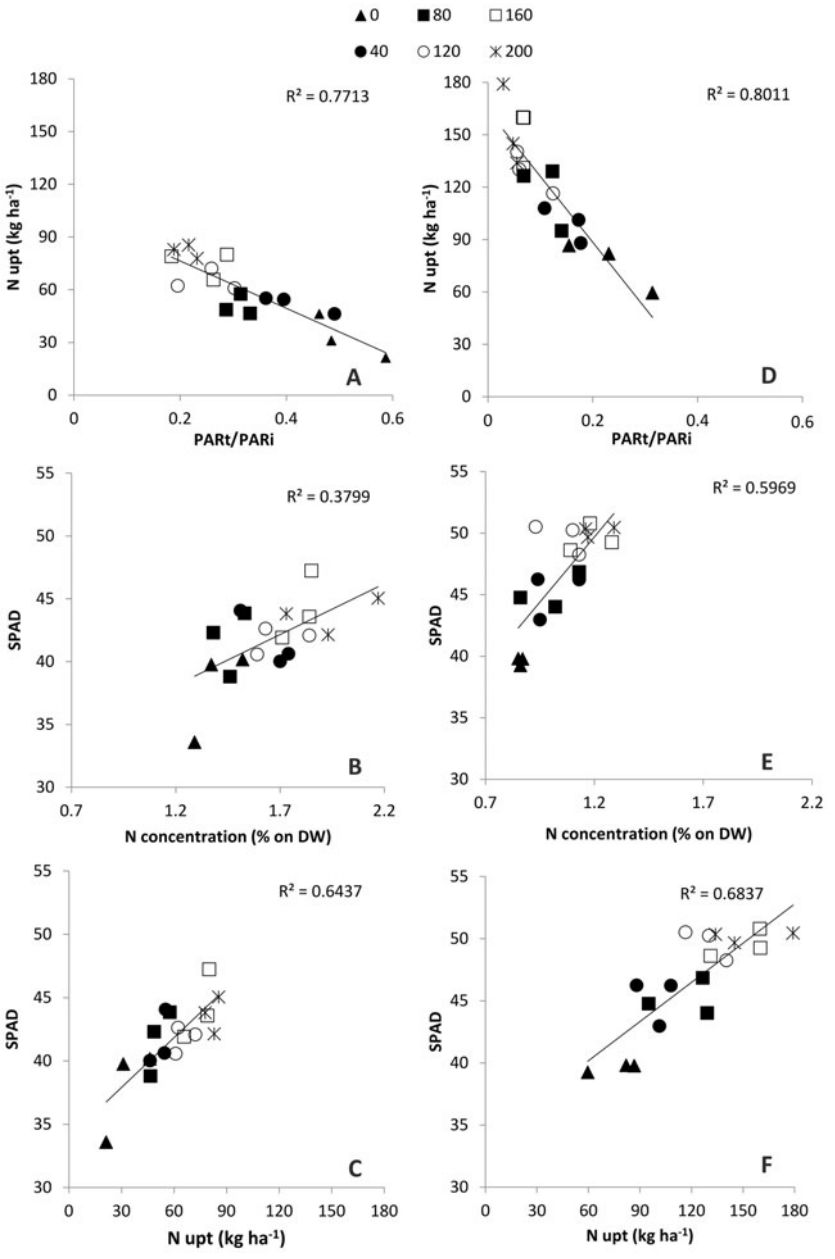

Figure 3. Relationships between in-field parameters measured to evaluate vegetative and N status of wheat grown at increasing N fertilization rates (0, 40, 80, 120, 160, 200 kg N ha^{-1}), split into two applications, the first at tillering (February 12th, 2015, 80 days after sowing, DAS) and the second at shooting (April 14th, 2015, 141 DAS). N% is the N concentration (w:w) in the above-ground dry matter, Nupt is the total above-ground N accumulation, SPAD readings express the leaf greenness, PARt is the photosynthetically active radiation transmitted to the soil below the canopy and PARi is the PAR incoming above the canopy. In A to C, measurements taken before the second fertilizer-N application (PARt/PARi and SPAD on April 1st, 128 DAS; N% and Nupt on April 14th). In D to F, measurements taken around one month after the second fertilizer-N application (PARt/PARi and SPAD on May 13th, 170 DAS; N% and Nupt on May 17th, 174 DAS).

https://doi.org/10.1017/S0014479717000278 Published online by Cambridge University Press

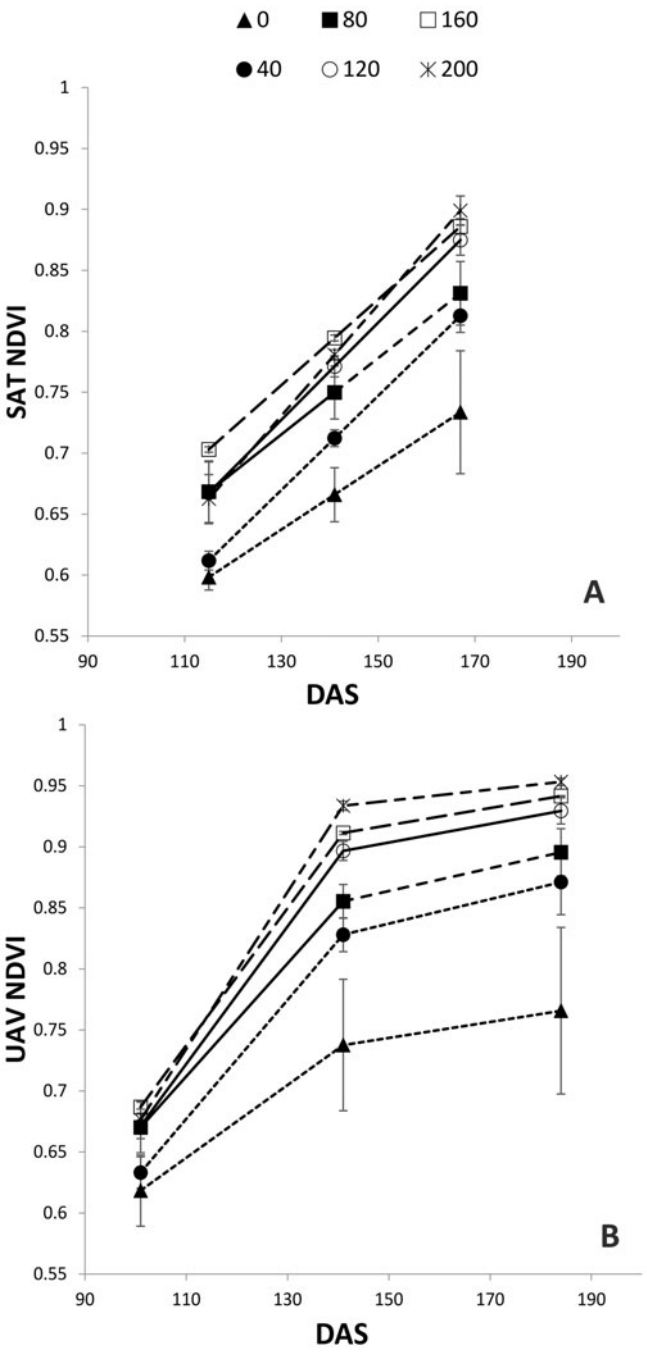

Figure 4. Time course of normalized difference vegetation index (NDVI) from (A) satellite (SAT) and (B) unmanned air vehicles (UAV) sensed data in soft wheat as affected by increasing N fertilization rates (0, 40, 80, 120, 160, 200 kg N ha^{-1}), split into two applications, the first at tillering (February 12th, 2015, 80 days after sowing, DAS) and the second at shooting (April 14th, 2015, 141 DAS). Vertical bars represent standard errors.

https://doi.org/10.1017/S0014479717000278 Published online by Cambridge University Press

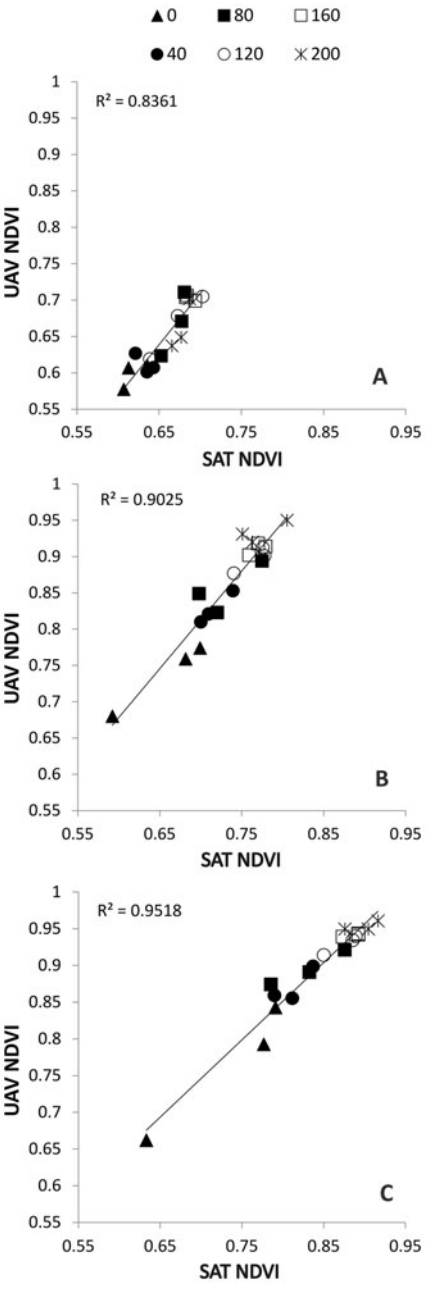

Figure 5. Relationships between UAV and SAT NDVI in wheat grown at increasing N fertilization rates (0, 40, 80, 120, 160, 200 kg N ha^{-1}) split into two applications, the first at tillering (February 12th, 2015, 80 days after sowing, DAS) and the second at shooting (April 14th, 2015, 141 DAS). In A, UAV NDVI recorded on March 31st (127 DAS) and SAT NDVI recorded on March 18th (114 DAS). In B, UAV NDVI recorded on April 14th and SAT NDVI of April 14th, calculated by linear interpolation between data recorded on March 18th and May 10th (167 DAS). In C, UAV NDVI recorded on May 18th (175 DAS) and SAT NDVI recorded on May 10th.

https://doi.org/10.1017/S0014479717000278 Published online by Cambridge University Press

Table 2. Pearson's R^2 and P values for the linear correlations between either UAV (unmanned aerial vehicle) NDVI (normalized difference vegetation index) or SAT (satellite) NDVI and in-field parameters measured to evaluate vegetative and N status in wheat grown with 0, 40, 80, 120, 160, 200 kg N ha^{-1}, split into two applications, the first at tillering (February 12th, 2015, 80 days after sowing, DAS), the second at shooting (April 14th, 2015, 141 DAS). PARt is the photosynthetically active radiation transmitted to the soil below the canopy and PARi is the PAR incoming above the canopy; N% is the nitrogen concentration (w:w) in the above-ground dry matter; Nupt is the total above-ground N accumulation; SPAD readings express the leaf greenness. Each correlation considers 18 points (6 N rates × 3 replicates). The closest measurement dates for in-field parameters and NDVI are compared. The SAT NDVI of April 14th is calculated by linear interpolation between data recorded on March 18th and May 10th.

		UAV (April 14th)		SAT (April 14th)	
In-field parameter	Measurement date	R^2	*p value*	R^2	*p value*
PAR_t/PAR_i	Apr 1st	0.8792	9.44E–09	0.7932	7.3E–07
N%	Apr 14th	0.5785	2.48E–04	0.4062	4.4E–03
Nupt	Apr 14th	0.8842	6.70E–09	0.7388	4.9E–06
SPAD	Apr 1st	0.7028	1.39E–05	0.6186	1.1E–04
		UAV (May 18th)		SAT (May 10th)	
		R^2	*p value*	R^2	*p value*
PAR_t/PAR_i	May 13th	0.9436	2.06E–11	0.9148	5.67E–10
N%	May 27th	0.5636	3.31E–04	0.5939	1.82E–04
Nupt	May 27th	0.7209	8.35E–06	0.7409	4.55E–06
SPAD	May 13th	0.7538	3.00E–06	0.7174	9.25E–06

and PARt/PARi (R^2 around 0.88) followed by those of SAT NDVI versus PARt/PARi ($R^2 = 0.79$) and Nupt to ($R^2 = 0.74$), while the weakest were those with N% (R^2 0.58 for UAV NDVI and 0.41 for SAT NDVI), as shown in Table 2. At around mid-May (about 170 DAS, i.e., about one month after the second N application) differences in pairwise correlations of UAV NDVI and SAT NDVI versus in-field parameters decreased (Table 2). With respect to mid-April, the strength of correlations with PARt/PARi and SPAD increased considerably for both UAV and SAT NDVI, while that with Nupt decreased markedly for UAV NDVI and that with N% increased dramatically for SAT NDVI (Table 2).

The correlation between grain yield and either UAV or SAT NDVI was weak for March data (R^2 below 0.5 for both), strong for April data ($R^2 = 0.80$ for UAV and 0.76 for SAT) and still reasonable for May data ($R^2 = 0.67$ for UAV and 0.68 for SAT) (Figure 6).

DISCUSSION

Our experimental design was able to differentiate the vegetative and nutritional status imposed with increasing N rates (Figure 1). In particular, the crop grown at the highest N rate had much higher leaf area than the unfertilized control. For example, assuming a hypothetical light extinction coefficient for wheat of 0.5 (Zhang *et al.*, 2015), the LAI was higher than five for the well N fed treatments and lower than two for the unfertilized control, as it can be easily derived from PARt/PARi values

https://doi.org/10.1017/S0014479717000278 Published online by Cambridge University Press

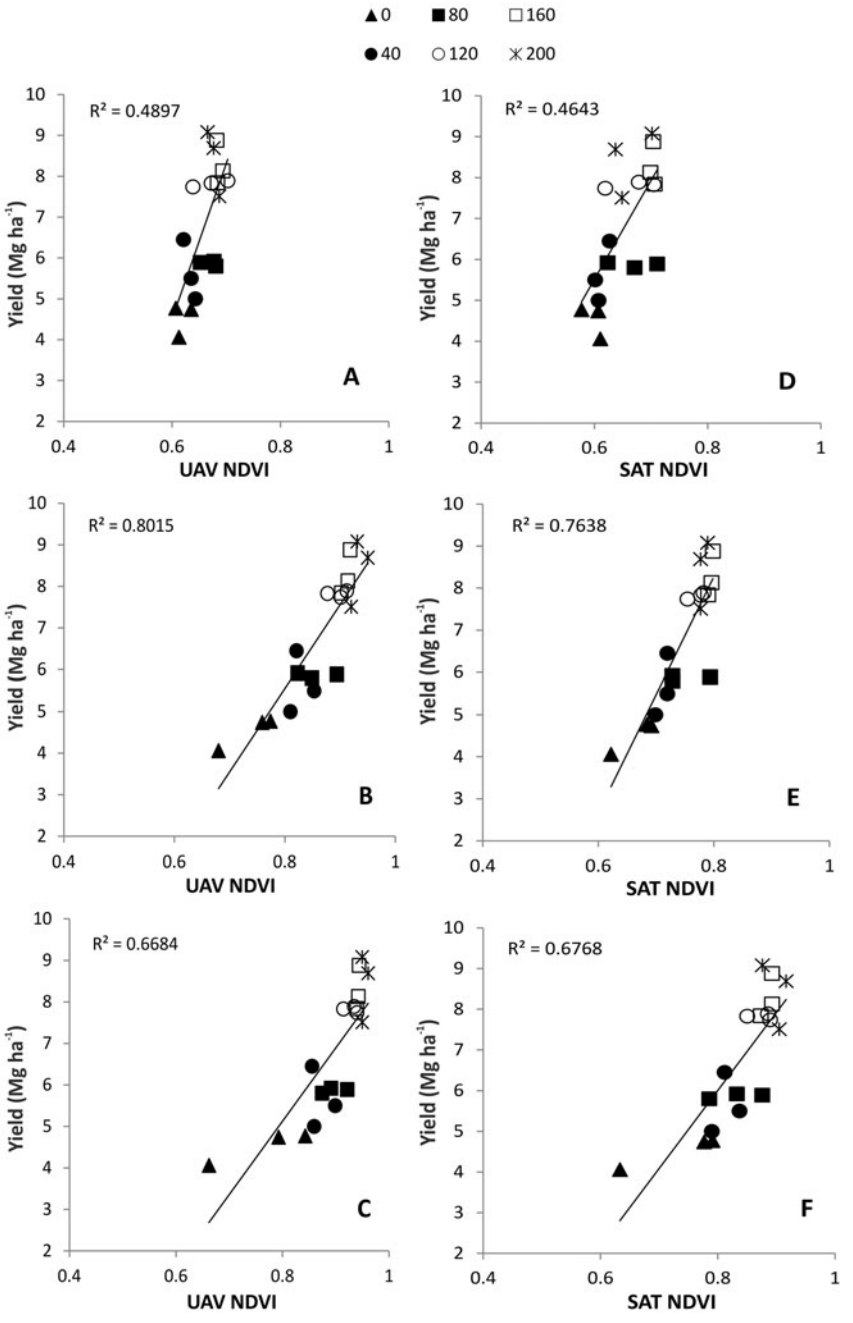

Figure 6. Correlations between either UAV (unmanned aerial vehicle) NDVI (normalized difference vegetation index) recorded on March 31st (127 days after sowing, DAS) (A), April 14th (141 DAS) (B) and May 18th (175 DAS) (C), or SAT (satellite) NDVI of March 18th (114 DAS) (D), April 14th (E) and May 10th (167 DAS) (F) and grain yield in soft wheat grown at increasing N fertilization rates (0, 40, 80, 120, 160, 200 kg N ha^{-1}), split into two applications, the first at tillering (February 12th, 2015, 80 DAS) and the second at shooting (April 14th, 2015). SAT NDVI of April 14th was calculated by linear interpolation between data recorded on March 18th and May 10th.

https://doi.org/10.1017/S0014479717000278 Published online by Cambridge University Press

according to the light penetration model proposed by Monsi and Saeki (1953). In turn, the higher leaf area index implied a higher soil cover and thus a lower bare soil component, which is known to affect the NDVI (Carlson and Ripley, 1997). Overall, based on differences between treatments visible in Figure 1, PARt/PARi and Nupt can be considered good indicators of wheat N availability, followed by SPAD and N% (Figure 1). In fact, since an N limited crop shows less biomass accumulation and leaf expansion, it is obvious and well documented in the literature that N concentration per unit biomass weight or unit leaf area (thus, N% and SPAD values) is less affected. Moreover, for a given N% concentration, some variation in SPAD values has been found due to differences in irradiance (Hoel and Solhaug, 1998), which is affected by solar elevation (thus on daytime and month), leaf angle and weather (e.g., haze, clouds). In any case, parameters taken by independent measurements like PARt/PARi, Nupt and SPAD resulted quite strongly correlated to each other (Figure 3), which means that each of them can be used to evaluate the accuracy of SAT and UAV NDVI.

Our results on NDVI (Figure 4) are in line with evidence obtained in Pakistan by Sultana *et al.* (2014), with some differences in absolute values likely associated with wheat cultivar and techniques used for spectral calibration. A slight UAV NDVI saturation occurred only for May data at the highest N rates, confirming the findings of Hansen and Schjoerring (2003), who concluded that some effect of saturation can occur for LAI higher than 2.5 and high N status. As the scientific literature suggests a linear variation of NDVI between tillering and booting growth stages, we performed a linear interpolation of satellite data that represents a simplistic predictor of values. This, together with the different calibration procedures of the data from the two satellite sensors, may have caused the reduction of SAT NDVI values on April 14th (141 DAS, Figure 4). However, this did not affect substantially the relative values of data and their correlations, so that the data could be used for in-field nitrogen assessment.

The little difference in SAT NDVI in fertilized treatments reflected the actual little difference in wheat N status caused by the unusually high winter rainfall that likely leached most of the N provided by the first N application. This is confirmed by the N concentration measured just before the second N application, which was markedly lower than the critical N concentration in all treatments (Figure 2). On the contrary, both SAT and UAV NDVI for high N rates were close to saturation several weeks after the second N application both due to the higher LAI and the improved N status, which was close to the critical N concentration (Figures 1, 2 and 4). However, the strong correlation between SAT and UAV NDVIs (Figure 5) indicates that, despite the two remote sensing methods imply different image pre-processing procedures, they have similar sensitiveness in monitoring crop vegetative/nutritional status and thus can be used alternatively for the assessment of in-field crop condition. Of course, the choice will depend on the peculiarities of each method, taking into account the context where to use it (e.g., cost, flexibility, weather conditions, land size, etc.) and the purpose of the assessment (e.g., cross-comparison with other fields, in field assessment etc.). For example, the use of SAT was not as flexible as that of UAV, and,

actually, we did not have the chance to make an additional/delayed measurement of NDVI with respect to that planned in mid-March. Moreover, considering that data from UAV can be calibrated through different approaches, the purpose of data collection should guide the calibration techniques to find a good compromise between the inter-comparability of data and the complexity of the calibration process.

The strength of correlations between either UAV or SAT NDVI and some in-field parameters was comparable to that of other widely recognized accurate systems (Cao *et al.*, 2015). The strong correlations of UAV and SAT NDVI with PARt/PARi (Table 2) support our previous statement that the NDVI was highly dependent on leaf area and ground cover. So, NDVI is an expression of the overall vegetative status rather than of the sole nutritional status of the crop. Similarly, the strong correlation between NDVI and Nupt (Table 2) was also due to the strong correlation of NDVI with DW (R^2 always >70%, data not shown) rather than with N%, confirming the findings of Jia *et al.* (2012). Thus, NDVI would be only in part able to screen an N deficient crop from a well N fed crop limited by other unfavourable environmental conditions (e.g., flooding, low temperature, etc.). This depends from the fact that the robustness and sensitivity of NDVI depends not only on vegetation red/infrared ratio related to greenness but also on ground cover by the canopy (Ren *et al.*, 2008). Actually, moderate N deficiency not always causes detectable changes in N concentrations per unit dry weight or unit leaf area and greenness (thus N% and SPAD values). Thus, the farmer should also consider possible unfavourable environmental conditions other than N availability for low NDVI when deciding whether adjust the N rate.

Data indicate that NDVI was able to screen quite well the crop vegetative/nutritional status in mid-April, i.e., at wheat shooting (Table 2). This is of relevance because at this stage there is still room for adjusting the N rate by the second N application. It is worth to notice that after the first N application the actual stepwise difference between N treatments was of just 20 kg N ha^{-1} (i.e., 0, 20, 40, 60, 80, 100 kg N ha^{-1}), which not necessarily has a detectable effect on crop vegetative and nutritional status. In addition, base soil N fertility likely accounted for some dozens of kg (explaining the quite high grain yield of the unfertilized control), which initially shifted the crop total N availability, thus contributing to mask effects of treatments. On the other hand, the heavy rainfall in March likely leached the N supplied with the first N application, so neutralising its effect. In fact, the in-field measurements themselves (N%, Nupt, and SPAD) revealed that contiguous N treatments were not so different. From an agronomic point of view, substantial differences were those between N deficient and well N fed clusters of treatments (e.g., 0–40 vs. 60–100 kg N ha^{-1}, before the second N application). These clusters were screened with due accuracy by either in-field methods or NDVIs.

The quite strong correlation between grain yield and NDVI of April (Figure 6) confirms that NDVI could be a good predictor of crop yield in wheat grown at a given N availability (Raun *et al.*, 2001), provided the N application has been efficient. The weak correlation of grain yield with March NDVI data is partly due to the above mentioned high rainfall, which likely leached most of the N supplied in mid-February.

https://doi.org/10.1017/S0014479717000278 Published online by Cambridge University Press

On the other hand, the slight decrease of accuracy of NDVI in May was caused by the above discussed saturation of NDVI at high N rates, as also shown by Lelong *et al.* (2008). However, the decrease of accuracy of NDVI at high N rates would have a relative importance because the gain in grain yield at high N availability becomes non-significant (Table 1). The lack of statistical difference between high N rates in terms of grain yield would indicate that the N concentration for maximum yield may be lower than N concentration for maximum growth. This stands especially for wheat, which has high crop plasticity and can compensate yield limitations at different crop stages, from tillering to grain filling.

CONCLUSIONS

Our results demonstrate that both UAV and SAT NDVIs are comparable to in-field methods for accuracy in detecting differences in crop N status and yield. In other words, remote sensed NDVI can be useful to reveal important N deficiencies and can detect this deficiency at an early crop stage like shooting, when the N rate can still be adjusted by a further fertilizer-N application. This means that NDVI derived from remote sensing can support a decision on whether and, to a certain extent, how much N rate has to be adjusted. This feature together with the chance of monitoring wide areas in little time allows fertilization according to crop spatial variability, thus improving fertilization management at a farm scale. The SAT and UAV NDVIs were strongly correlated to each other and then they can be used alternatively for the assessment of crop nitrogen status, depending on the context where to use them (e.g., cost, flexibility, weather, land size, etc.). An accurate timing of remote sensing image acquisition is highly recommended to obtain relevant information for N management purposes.

Acknowledgements. We gratefully acknowledge Mr. Daniele Luchetti and all workers of the FIELD-LAB of the Department of Agricultural, Food and Environmental Sciences in Papiano for their help in the agronomic management and plant sampling. This research was funded by the Project S.I.G. (Sistema Informativo Geografico a supporto della precision farming) PSR 2007–2013 Mis. 1.2.4. of Umbria Region. The experiment was hosted by the Foundation for Agricultural Education of the University of Perugia.

SUPPLEMENTARY MATERIAL

For supplementary material for this article, please visit https://doi.org/10.1017/S0014479717000278.

REFERENCES

Basso, B., Ritchie, J. T., Pierce, F. J., Braga, R. P. and Jones, J. W. (2001). Spatial validation of crop models for precision agriculture. *Agricultural Systems* 68:97–112.

Benincasa, P., Farneselli, M., Tosti, G., Bonciarelli, U., Lorenzetti, M. C. and Guiducci, M. (2016). Eleven-year results on soft and durum wheat crops grown in an organic and in a conventional low input cropping system. *Italian Journal of Agronomy* 11:77–84.

Bonciarelli, U., Onofri, A., Benincasa, P., Farneselli, M., Guiducci, M., Pannacci, E., Tosti, G. and Tei, F. (2016). Long-term evaluation of productivity, stability and sustainability for cropping systems in Mediterranean rainfed conditions. *European Journal of Agronomy* 77:146–155.

Bongiovanni, R. and Lowenberg-Deboer, J. (2004). Precision agriculture and sustainability. *Precision Agriculture* 5:359–387.

Bora, G. C., Nowatzki, J. F. and Roberts, D. C. (2012). Energy savings by adopting precision agriculture in rural USA. *Energy, Sustainability and Society* 2:1, 22, 5.

Bouvet, M. (2014). Radiometric comparison of multispectral imagers over a pseudo-invariant calibration site using a reference radiometric model. *Remote Sensing of Environment* 140:141–154.

Campbell, J. B. and Wayne, R. H. (2011). *Introduction to Remote Sensing* (5th ed). New York: The Guildford Press.

Candiago, S., Remondino, F., De Giglio, M., Dubbini, M. and Gattelli, M. (2015). Evaluating multispectral images and vegetation indices for precision farming applications from UAV images. *Remote Sensing*. 7:4026–4047.

Cao, Q., Miao, Y., Feng, G., Gao, X., Li, F., Liu, B., Yue, S., Cheng, S., Ustin, S. L. and Khosla, R. (2015). Active canopy sensing of winter wheat nitrogen status: An evaluation of two sensor systems. *Computers and Electronics in Agriculture* 112:54–67.

Carlson, T. and Ripley, D. A. (1997). On the relation between NDVI, fractional vegetation cover, and leaf area index. *Remote Sensing of Environment* 62:241–252.

Casa, R. and Castrignanò, A. (2008). Analysis of spatial relationships between soil and crop variables in a durum wheat field using a multivariate geostatistical approach. *European Journal of Agronomy* 28:331–342.

De la Casa, A. C. and Ovando, G. G. (2013). Estimation of Wheat Area in Córdoba, Argentina, with Multitemporal NDVI Data of SPOT-Vegetation. *International Journal of Geosciences* 4:1355–1364.

Eitel, J. U. H., Vierling, L. A., Long, D. S. and Hunt, E. R. (2011). Early season remote sensing of wheat nitrogen status using a green scanning laser. *Agricultural and Forest Meteorology* 151:1338–1345.

Hadjimitsis, D. G., Clayton, C. R. I. and Retalis, A. (2009). The use of selected pseudo-invariant targets for the application of atmospheric correction in multi-temporal studies using satellite remotely sensed imagery. *International Journal of Applied Earth Observation and Geoinformation* 11:192–200.

Hansen, P. M. and Schjoerring, J. K. (2003). Reflectance measurement of canopy biomass and nitrogen status in wheat crops using normalized difference vegetation indices and partial least squares regression. *Remote Sensing of Environment* 86:542–553.

Hoel, B. O. and Solhaug, K. A. (1998). Effect of irradiance on chlorophyll estimation with the Minolta SPAD-502 leaf cholorophyll meter. *Annals of Botany* 82:389–392.

Honkavaara, E., Hakala, T., Markelin, L. and Peltoniemi, J. (2014). Metrology of image processing in spectral reflectance measurement by UAV. *International Archives of the Photogrammetry, Remote Sensing and Spatial Information Sciences* 40:53–58.

Huete, A. R., Liu, H. Q., Batchily, K. and van Leeuwen, W. (1997). A comparsion of vegetation indices over a Global set of TM images for EO -MODIS. *Remote Sensing of Environment* 59:440–451.

Jia, L., Yu, Z., Li, F., Gnyp, M., Koppe, W., Bareth, G., Miao, Y., Chen, X. and Zhang, F. (2012). Nitrogen Status Estimation of Winter Wheat by Using an IKONOS Satellite Image in the North China Plain. *Computer and Computing Technologies in Agriculture* 369:174–184.

Lelong, C. C. D., Burger, P., Jubelin, G., Roux, B., Labbé, S. and Baret, F. (2008). Assessment of unmanned aerial vehicles imagery for quantitative monitoring of wheat crop in small plots. *Sensors* 8:3557–3585.

Maresma, Á., Ariza, M., Martínez, E., Lloveras, J. and Martínez-Casasnovas, J. (2016). Analysis of Vegetation Indices to Determine Nitrogen Application and Yield Prediction in Maize (Zea mays L.) from a Standard UAV Service. *Remote Sensing* 8:973.

Monsi, M. and Saeki, T. (1953). The light factor in plant communities and its significance for dry matter production. *Japanese Journal of Botany* 14:22–52.

Muñoz-Huerta, R. F., Guevara-Gonzalez, R. G., Contreras-Medina, L. M., Torres-Pacheco, I., Prado-Olivarez, J. and Ocampo-Velazquez, R. V. (2013). A review of methods for sensing the nitrogen status in plants: Advantages, disadvantages and recent advances. *Sensors* 13:10823–10843.

Perry, E., Morse-Mcnabb, E., Nuttall, J., O'Leary, G. and Clark, R. (2013). Managing wheat from space: Linking MODIS NDVI and crop models for Australian dryland wheat. *International Geoscience and Remote Sensing Symposium* 7:3243–3245.

QGIS Development Team (2014). No Title. QGIS Geographic Information System. Open Source Geospatial Foundation Project. Available at: http://qgis.osgeo.org.

Quebrajo, L., Pérez-Ruiz, M., Rodriguez-Lizana, A. and Agüera, J. (2015). An Approach to Precise Nitrogen Management Using Hand-Held Crop Sensor Measurements and Winter Wheat Yield Mapping in a Mediterranean Environment. *Sensors* 15:5504–5517.

Raun, W. R., Solie, J. B., Johnson G, V., Stone, M. L., Lukina, E. V., Thomason, W. E. and Schepers, J. S. (2001). In-season prediction of potential grain yield in winter wheat using canopy reflectance. *Agronomy Journal* 93:131.

Ren, J., Chen, Z., Zhou, Q. and Tang, H. (2008). Regional yield estimation for winter wheat with MODIS-NDVI data in Shandong, China. *International Journal of Applied Earth Observation and Geoinformation* 10:403–410.

Saberioon, M. M., Amin, M. S. M., Anuar, A. R., Gholizadeh, A., Wayayok, A. and Khairunniza-Bejo, S. (2014). Assessment of rice leaf chlorophyll content using visible bands at different growth stages at both the leaf and canopy scale. *International Journal of Applied Earth Observation and Geoinformation* 32:35–45.

Sultana, S. R., Ali, A., Ahmad, A., Mubeen, M., Ahmad, S., Ercisli, S. and Jaafar, H. Z. E. (2014). Normalized Difference vegetation index as a tool for wheat yield estimation: A case study from Faisalabad, Pakistan. *The Scientific World Journal* 2014, ID 725326, 8 p.

Tei, F., Benincasa, P. and Guiducci, M. (2003). Critical nitrogen concentration in lettuce. *Acta Horticulturae* 627:227–232.

Thenkabail, P. S., Smith, R. B. and De Pauw, E. (2000). Hyperspectral vegetation indices and their relationships with agricultural crop characteristics. *Remote Sensing of Environment* 71:158–182.

Tilling, A. K., O'Leary, G. J., Ferwerda, J. G., Jones, S. D., Fitzgerald, G. J., Rodriguez, D. and Belford, R. (2007). Remote sensing of nitrogen and water stress in wheat. *Field Crops Research* 104:77–85.

Torres-Sánchez, J., Peña, J. M., de Castro, A. I. and López-Granados, F. (2014). Multi-temporal mapping of the vegetation fraction in early-season wheat fields using images from UAV. *Computers and Electronics in Agriculture* 103:104–113.

Ulissi, V., Antonucci, F., Benincasa, P., Farneselli, M., Tosti, G., Guiducci, M., Tei, F., Costa, C., Pallottino, F. and Menesatti, P. (2011). Nitrogen content estimation on tomato leaves by VIS-NIR non-destructive spectral reflectance system. *Sensors* 11:6411–6424.

Vermote, E. F., Tanre, D., Deuze, J. L., Herman, M. and Morcrette, J. J. (1997). Second simulation of the satellite signal in the solar spectrum, 6S: An overview. *IEEE Transactions on Geoscience and Remote Sensing* 35:675–686.

Wu, B., Gommes, R., Zhang, M., Zeng, H., Yan, N., Zou, W., Zheng, Y., Zhang, N., Chang, S., Xing, Q. and van Heijden, A. (2015). Global Crop Monitoring: A Satellite-Based Hierarchical Approach. *Remote Sensing* 7: 3907–3933.

Zhang, W., Tang, L., Yang, X., Liu, L., Cao, W. and Zhu, Y. (2015). A simulation model for predicting canopy structure and light distribution in wheat. *European Journal of Agronomy* 67:1–11.